Chapter 4

Imaging of Insulin Exocytosis from Pancreatic Beta Cells

Mica Ohara-Imaizumi, Kyota Aoyagi, and Shinya Nagamatsu

Abstract

The pancreatic beta cells are highly sensitive to the glucose concentration, and the minute to minute regulation of insulin secretion by glucose occurs at the level of exocytosis of insulin, transcriptional rate of the insulin gene, translation of the mRNA, and processing of the proinsulin to mature insulin (Mahato et al., Biochem J 174:517–526, 1978; Hedeskov, Physiol Rev 60:442–509, 1980; Welsh et al., J Biol Chem 260:13590–13594, 1985; Welsh et al., Biochem J 235:459–467, 1986; Newgard and McGarry, Annu Rev Biochem 64:689–719,1995). Thus, glucose is the most important physiological regulator of insulin gene transcription, biosynthesis, and secretion. The insulin biosynthetic rate is not always proportional to the secretion rate. Insulin secretion occurs by the fusion of insulin granules and plasma membrane (Nagamatsu, Pancreatic beta cells in health and disease 177–194, 2008). Insulin granules exist as large–dense core structures that are discernible by electron microscopy as an electron-dense interior surrounded by a clear region in a 300–350-nm intracellular membrane-delineated compartment (Greider et al., J Cell Biol 41:162–166, 1969; Lange, J Ultrastruct Res 46:301–307, 1974).

It is generally accepted that SNARE proteins play a crucial role in insulin exocytotic process (Wollheim et al, Diabetes Rev 4:276–297, 1996). Several reports revealed that t-SNARE protein syntaxin 1(syt1) and SNAP-25 are plasma membrane localized, whereas the v-SNARE protein VAMP2 is associated with insulin secretory granules (Regazzi et al., EMBO J 14:2723–2730, 1995; Sadoul et al., J Cell Biol 128:1019–1028, 1995; Boyd et al., J Biol Chem 270:18216–18218, 1995; Nagamatsu et al., J Biol Chem 271:1160–1165, 1996). Furthermore, we previously reported that alteration of SNARE proteins expression is closely associated with type 2 diabetes (Nagamatsu et al., Diabetes 48:2367–2373, 1999; Ohara-Imaizumi et al., Diabetologia 47:2200–2207, 2004). In order to explore the mechanism of insulin exocytosis, methods for gene transfer and imaging system are powerful tools. Here, we describe about the methods for studying the insulin exocytosis from the point of view of imaging techniques and gene transfer system.

Key words Exocytosis, Insulin, Electroporation, Fluorescence, TIRF

1 A New Electroporation System Gene Transfer System in Pancreatic Beta Cells

1.1 Introduction

Gene transfection is a powerful tool to study the functional role of proteins in the glucose-induced insulin secretion. Due to their capacity to mediate highly efficient gene transfer in nondividing cells, virus-mediated gene transfer has emerged as the first choice for engineering beta cells. Together with Lentiviruses [16] and adeno-associated viruses [17], adenoviruses are the most

Peter Thorn (ed.), *Exocytosis Methods*, Neuromethods, vol. 83,
DOI 10.1007/978-1-62703-676-4_4,

commonly used viral vectors in current beta-cell research [18]. Because of their high transfection efficacy, the amount of secreted insulin from recombinant virus-infected islets is widely used to evaluate the effect of transgene on the insulin secretion from infected beta cells. However, adenoviruses can infect not all but only a subpopulation of beta cells in pancreatic islets. Thus, the amount of secreted insulin from recombinant virus-infected islets should consist of that from infected and uninfected beta cells in infected islets, which results in the underestimation of the effect of transgene expression.

To circumvent of this problem, human growth hormone (hGH) is widely used as a transfection reporter [19]. In many cell types, exogenously expressed hGH is shown to be stored in secretory vesicles and secreted into extracellular medium in response to stimulation; thus, the measurement of secreted hGH can be used to evaluate the secretion only from transfected cells. Indeed, in beta-cell-derived cell lines, INS-1 and Min6 cells, co-transfection of hGH with a gene of interest by lipofection and evaluation of secreted hGH to examine the effect of transgene on secretion is commonly used [20, 21]. However, it is technically difficult for adenoviruses to transfer two independent transgene simultaneously. Nonviral methods are commonly used for co-transfection in several cell types, but their transfection efficacies in pancreatic islets are very low [22–24] because pancreatic islets are terminally differentiated cell clusters that are difficult to introduce exogenous plasmids.

Here, we described a new transfection system based on electroporation, which enables us to co-transfect hGH and a gene of interest and thereby assess the effect of transgene on the glucose-induced secretion. Our method uses standard plasmids to introduce transgene, which will cut down the time needed to produce recombinant adenoviruses, thus accelerates projects to elucidate the beta-cell functions.

1.2 Materials and Methods

1.2.1 Overview of Islet Electroporation

Freshly isolated pancreatic islets are suspended in Hank's balanced salt solution (HBSS) (Invitrogen). To prevent islets from adhering to manipulating pipette and electrode chamber, 0.5 % BSA is supplemented in the HBSS. We confirmed that 0.5 % BSA did not affect transfection efficacy and islet viability. Islets are transferred into an open electrode chamber (CUY520P5, Nepa gene, Chiba, Japan) filled with 0.5 % BSA-containing HBSS supplemented with plasmid DNA at a concentration of 1.0–1.5 mg/ml. To increase the transfection efficacy, aggregated islets should be dispersed by pipetting. After application of electric pulses, islets are handpicked using pipette and suspended into culture medium. After two times wash with culture medium, electroporated islets are placed in 35- or 60-mm culture dish (Iwaki, Tokyo, Japan) and cultured for 2 days.

1.2.2 DNA Concentration

High plasmid DNA concentration will result in high transfection efficacy. On the other hand, high DNA concentration will generate big sticky materials mainly made from DNA on the surface of the anode, which will entangle islets and result in severe difficulty in islet recovery from the electrode chamber after electroporation. Therefore, DNA solution at a concentration of 1.0–1.5 mg/ml is usually used for our electroporation. Plasmid DNA is prepared using Qiagen Mega or Giga prep kit (Qiagen) and dissolved into TE at a concentration of >8 mg/ml for stock. Quality of plasmid DNA severely affects the transfection efficacy. The plasmid DNA prepared by CsCl centrifugation followed by phenol/chloroform extraction reduces the transfection efficacy in our procedure.

1.2.3 Number of Islets for Electroporation

The number of islets subjected to electroporation does not affect the transfection efficacy if they are not aggregated. However, if too much islets are used for one electroporation, a part of islets will be lost by sticking the DNA-containing materials on the surface of the anode. Therefore, to avoid the deprivation of islets, 100–150 islets are usually used for one electroporation.

1.2.4 Electric Pulse Setting

Nepa21 pulse generator (Nepa gene) is used to apply electric pulses. This pulse generator enables to apply electric pulses with two distinct settings. For islet electroporation, short, high-voltage pulses (poring pulses) are applied to break the plasma membrane and form small pores, and then plasmid DNA is introduced into islet cells by long, low-voltage pulses (transfer pulses). The settings of transfer pulses have little impact on transfection efficacy and islet viability. We observed that the voltage (50–80 V) and pulse length (50–70 ms) did not affect the transfection efficacy. On the other hand, the poring pulse setting dramatically affects the transfection efficacy and islet viability. In order to optimize the poring pulse setting, we examined the relationship between the voltages of poring pulses and the amount of exogenously expressed hGH in transfected islets. In the experiments, various voltage pulses (6 pulses, decay constant (10 %), pulse interval (50 ms)) were applied as poring pulses and the amount of hGH expressed in electroporated islets was measured by ELISA (Roche) 2 days after electroporation. As shown in Fig. 1, the amount of expressed hGH showed bell-shaped relationship against the 1 ms poring pulses. On the other hand, the amount of expressed hGH was inversely correlated with the voltages of 2.5 ms poring pulses. In these experiments, we found that application of poring pulses at 200 V for 2.5 ms resulted in the highest expression of hGH, but we also found that isolated islets were seriously damaged by 2.5 ms pulses. As for the 1 ms pulses, 220 V gave higher expression of hGH than 200 V, but electroporated islets with 200 V pulses looked better than those with 220 V. From these results, we apply six pulses (200 V, 1 ms duration, 50 ms interval, decay constant (10 %)) as

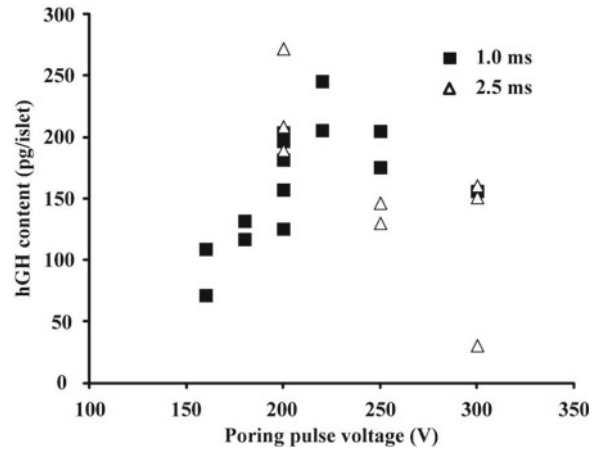

Fig. 1 Relationship between poring pulse setting and the amount of exogenously expressed hGH. Size-matched pancreatic islets were subjected to 1.0-ms (*filled rectangle*) or 2.5-ms (*open triangle*) poring pulse with indicated voltages, and the amounts of hGH were determined by ELISA 2 days after electroporation

poring pulses followed by five pulses (50 V, 50 ms duration, 50 ms interval, decay constant (40 %)) and another five pulses in the opposite direction of the electric field as transfer pulses.

1.2.5 Western Blotting Analysis of Exogenously Expressed Gene

To examine whether the exogenously expressed gene can be expressed in electroporated islets, we performed western blotting. Freshly isolated islets were electroporated with a plasmid encoding V5-tagged human Arf6 (Arf6-V5) or a mock vector and cultured for 2 days. Seventy-five electroporated islets were washed with KRB containing 2.2 mM glucose and recovered in 50 μl of sample buffer (2 % (w/v) SDS, 10 % (w/v) sucrose, 0.05 % (w/v) Bromophenol blue, 62.5 mM Tris–HCl, pH 7.4) supplemented with 20 μM DTT. Sodium dodecyl sulfate (SDS)-polyacrylamide gel electrophoresis (PAGE) was performed on 11 % polyacrylamide gel equipped with 5 % stacking gel. After separation of 20 μl of the sample by SDS-PAGE, the proteins were transferred to polyvinylidene difluoride (PVDF) membranes following standard procedures with a semidry transblotting apparatus. The membrane was blocked in 5 % (w/v) nonfat milk in TBST (150 mM NaCl, 0.05 % (w/v) Tween 20, 25 mM Tris–HCl, pH 7.5) for 30 min at room temperature followed by overnight incubation with anti-V5 antibody (Invitrogen) diluted in Can Get Signal solution (TOYOBO, Tokyo, Japan). After washing in TBST, the membrane was incubated for 1 h at room temperature with horse radish peroxidase-labeled anti-mouse IgG (DAKO) in Can Get Signal solution. After washing, the immunoreactive bands were visualized by SuperSignal (PIERCE) and a luminescence image analyzer with

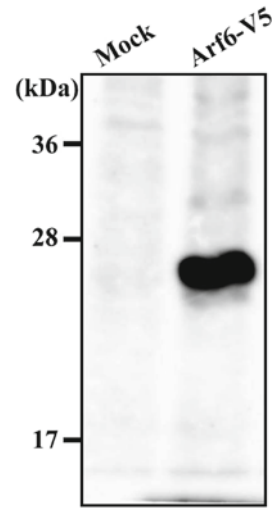

Fig. 2 Western blotting analysis in transfected islets. A mock vector or the vector encoding V5-tagged human Arf6 transfected islets were subjected to western blotting using anti-V5 antibody

an electronically cooled charge-coupled device camera system (LAS-4000, GE Healthcare). As shown in Fig. 2, a specific signal can be detected in Arf6-V5-transfected islets.

1.2.6 Identification of Transfected Islet Cell Types

Pancreatic islets consist of four different types of endocrine cells: insulin (β)-, glucagon (α)-, somatostatin (δ)-, and pancreatic polypeptide (PP)-producing cells. In mouse islets, alpha and beta cells are composed of 18 and 77 % of total islet cell population, respectively [25]. Thus, exogenous plasmid DNA will be introduced into these four types of cells by electroporation of islets and identification of cell type of transfected cells should be required. To this end, we examined which types of cells were transfected by our electroporation.

Electroporated islets with a plasmid encoding CMV promoter-driven EGFP (pEGFP-N1, Clontech) were dissociated into single cells by incubation in Ca^{2+}-free KRB containing 1 mM EGTA and cultured on fibronectin-coated (Koken Co., Tokyo, Japan) coverslips in RPMI1640 medium supplemented with 10 % FBS (Gibco BRL), 200 units/ml penicillin, and 200 μg/ml streptomycin at 37 °C in an atmosphere of 5 % CO_2.

Two days after electroporation, cells were fixed for 15 min at room temperature in 4 % paraformaldehyde (PFA) and washed three times in PBS for 5 min each. They were then incubated with the anti-insulin (Sigma) or anti-glucagon (Sigma) antibodies at 4 °C overnight, respectively. After washing three times with PBS for 5 min each, they were incubated with alexa546-tagged

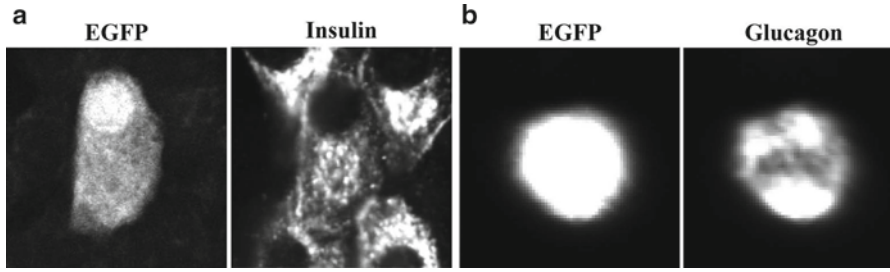

Fig. 3 Immunostaining of transfected islet cells. The CMV promoter-driven EGFP transfected islet cells were immunostained with anti-insulin and anti-glucagon antibody. About 50 % of EGFP positive cells were stained with anti-insulin antibody (**a**) and about 30 % of EGFP positive cells were immunostained with anti-glucagon antibody (**b**)

anti-mouse IgG (Invitrogen) at room temperature for 1 h, washed three times with PBS, and then mounted with DABCO. Immunostained islet cells were observed using confocal laser microscopy, FV1000 with a 40× 1.35 NA UApo objective (Olympus, Tokyo, Japan).

As shown in Fig. 3, we observed GFP-positive cells labeled with anti-insulin and anti-glucagon antibodies, respectively. By counting the number of GFP-positive cells, we found that about 50 and 30 % of transfected cells were insulin-positive β-cells and glucagon-positive α-cells, respectively.

1.2.7 Secretion Assay from Transfected β-Cells in Islets

In order to demonstrate that electroporated islets cultured for 2 days can maintain their function, we next examined the secretagogue-induced secretion in transfected islet cells. Because exogenously expressed human growth hormone was shown to be stored into insulin granule and to be secreted into extracellular medium by exocytosis in pancreatic beta-cell lines [20, 21], freshly isolated islets were electroporated with a plasmid encoding CMV promoter-driven hGH. Two days after electroporation, 15 size-matched islets were preincubated for 30 min in 500 μl of KRB containing 2.2 mM glucose and then transferred into 250 μl of KRB containing 2.2 or 16 mM glucose. After 30 min incubation, islets were removed by pipette and supernatant was recovered as the secreted sample. The picked islets were transferred into 1 ml of KRB containing 1 % Nonidet P-40 and 100 mM KCl, then sonicated on ice to recover the total cellular contents of insulin and hGH. The secreted and total cellular content of insulin and hGH were measured by an insulin ELISA kit (Morinaga, Japan) and a hGH ELISA kit (Roche). As shown in Fig. 4, 16 mM glucose, a physiological secretagogue for insulin from pancreatic beta cells, stimulated hGH secretion, indicating that β-cells in electroporated islets can maintain their function after 2 days cultivation.

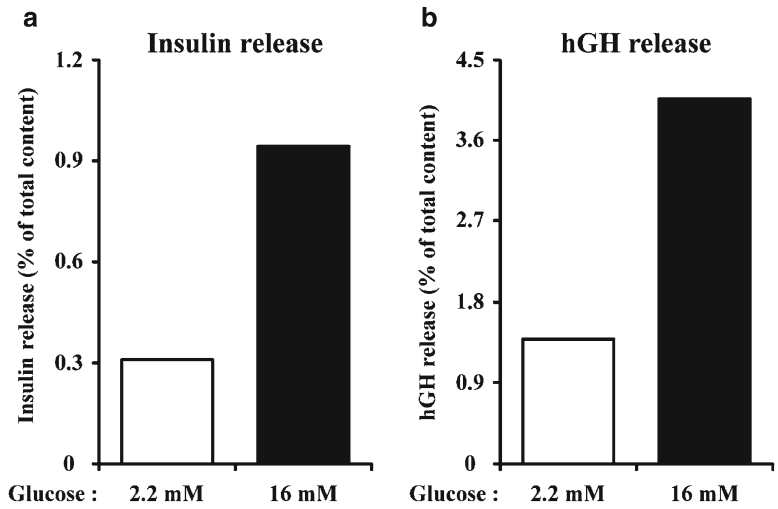

Fig. 4 An example of insulin/hGH secretion assay. Fifteen size-matched islets transfected with hGH were stimulated with 2.2 or 16 mM glucose for 30 min. The amount of insulin and hGH secreted from the same batch of islets was measured by ELISA. The amount of secreted insulin (**a**) and hGH (**b**) is expressed as the percentage of total cellular contents

Pancreatic beta cells show a characteristic biphasic insulin secretion consisting of a rapidly developing and transient first phase followed by a sustained second phase [26, 27]. To further examine whether transfected β-cells in electroporated islets can respond to the glucose stimulation, we next performed the perifusion assay to demonstrate biphasic hGH secretion in transfected beta cells. Freshly isolated islets were electroporated with the vector encoding the CMV promoter-driven hGH and cultured for 2 days. The size-matched 200 islet s were housed in a small chamber and perifused with KRB containing 2.8 mM glucose for 30 min at a flow rate of 0.3 ml/min. Insulin/hGH secretion was stimulated by 22 mM glucose for 30 min. After the experiments, islets were solubilized by 1 % Nonidet P-40 to recover the total cellular content of insulin and hGH. As show in Fig. 5, hGH secretion showed a biphasic pattern, which looks very similar to that of insulin secretion from the same batch of islets.

2 TIRF Imaging in Pancreatic Beta Cells

2.1 Introduction

TIRF microscopy is a technique that specifically illuminates fluorophores within a closely restricted layer just adjacent to the interface at which total internal reflection occurs [28, 29]. When angled light strikes the interface and the light undergoes total internal reflection, some of the light penetrates the

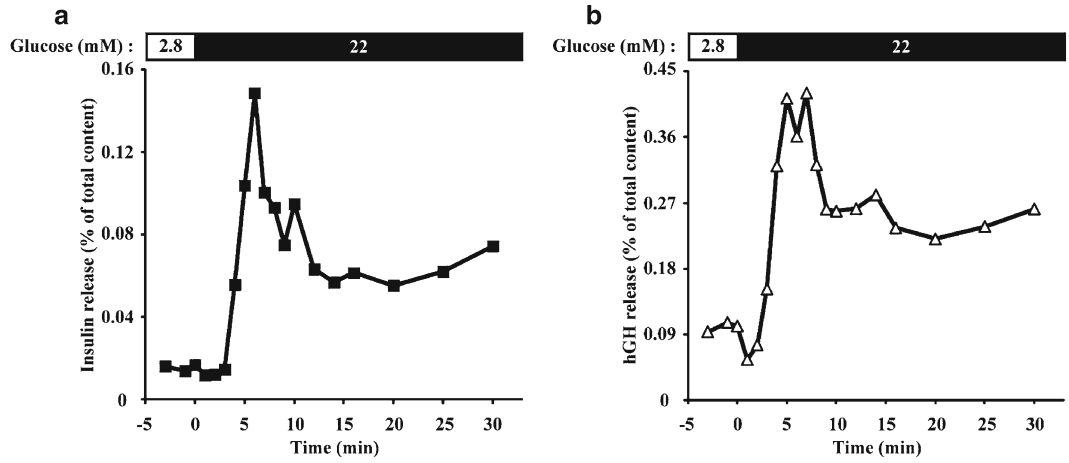

Fig. 5 An example of insulin/hGH perifusion assay. Two hundred of size-matched islets transfected with hGH were perifused with 2.8 or 22 mM glucose. The amount of insulin and hGH secreted from the same batch of islets was measured by ELISA. Both insulin (**a**) and hGH (**b**) showed the characteristic biphasic secretion pattern with almost the same time course. The amount of secreted insulin and hGH is expressed as the percentage of total cellular contents

interface as an electromagnetic field called "evanescent wave." Because the evanescent wave vanishes exponentially with distance from the interface, the penetration depth of the evanescent field is usually less than 100 nm (Fig. 6). Therefore, when cells are grown on a coverslip, a very thin layer adjacent to the coverslip can be specifically illuminated by the evanescent wave formed by the total internal reflection occurring at the interface between the coverslip and extracellular medium. In pioneering work by Daniel Axelrod, this technique was first applied to the study of live cells, primarily to investigate cell surface adhesions [30]. Then, several studies of protein dynamics, topography of cell–substrate contacts, endocytosis, and exocytosis using this technique were reported [31–36].

Because the exocytotic process occurs in the vicinity of the plasma membrane, TIRF microscopy is a powerful tool to analyze the exocytotic process of individual insulin granules in living pancreatic beta cells. To observe the insulin secretory process under TIRF microscopy, insulin granules should be labeled with fluorescent probes. Previously, a weak base fluorescent dye, acridine orange, was used for labeling granules because the inside of most vesicles is acidic [37]. However, acridine orange accumulates not only in insulin granules but also other secretory vesicles such as GABA-containing small synaptic-like vesicles. Thus, the expression of GFP-tagged insulin would be best to specifically analyze the motion of insulin granules. Therefore, we made a recombinant adenovirus encoding human preproinsulin tagged with GFP, which is localized in insulin secretory granules [38, 39], allowing us to

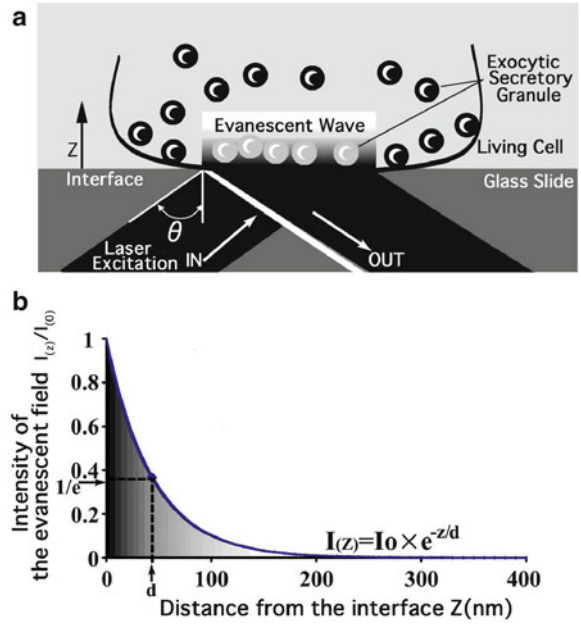

Fig. 6 TIRF excitation using an evanescent field. (**a**) Schematic drawing of the evanescent wave excitation. When a light beam propagating through a transparent medium of high refractive index n_1 (e.g., coverglass) encounters an interface with a medium of lower refractive index n_2 (e.g., adhering cells), total internal reflection occurs at incidence angles (θ), which are greater than critical angle. Although being totally reflected, some of the incident light beam evokes an evanescent field that penetrates into the medium of lower refractive index. (**b**) The intensity of the evanescent field exponentially decays with increasing distance from the interface: $I_{(z)} = I_{(0)}e^{-Z/d}$, where $I_{(z)}$ represents the intensity at a perpendicular distance z from the interface and $I_{(0)}$ is the intensity at the interface. The theoretical penetration depth (d: the distance where the intensity has decreased to $I_{(0)}/e$) depends on the incidence angle (θ), wavelength (λ), as well as the refractive index of the glass (n_1) and medium (n_2): $d = (\lambda/4\pi)(n_1^2 \sin^2\theta - n_2^2)^{-1/2}$. The penetration depth, which usually ranges 30–100 nm, decreases with increasing θ. For example, when a laser light ($\lambda = 488$ nm) propagates through the high-refractive-index glass ($n_1 = 1.8$) at the incidence angle ($\theta = 65^\circ$) onto the cells ($n_2 = 1.37$), d equals 44 nm calculated from the formula (see refs. [28, 29])

analyze the real-time motion of insulin granules (**Note 1**). We describe the methodology of TIRF microscopy in insulin exocytosis of pancreatic beta cells.

2.2 Materials

2.2.1 Probes Used for Labeling of Insulin Granules

1. Plasmids Used for Labeling of Insulin Granules in MIN6 Cells
   Human pre-proinsulin cDNA pchi 1–19 (provided by Professor G. I. Bell, University of Chicago, Chicago, IL, USA) lacking a TGA stop codon was amplified by PCR using forward primer, 5-*GAATTC*CGGGGGTCCTTCTGCCATG-3 (*Eco*RI site is italicized), and reverse primer, 5-*GGATCC*-CAGTTGCAGTAGTTCTCCAGC-3, where TGA was

replaced by TGG. The product was subcloned into a pGEMT easy vector (Promega, Madison, WI, USA). The approx. 0.3-kb insulin cDNA fragment lacking stop codon was cleaved by *Eco*RI and *Bam*HI double digestion, which was subcloned into the *Eco*RI and *Bam*HI site of multiple cloning sites of pEGFP-N1 (Clontech/Takara Bio, Otsu, Japan) [38].

2. Recombinant Adenovirus Used for Labeling of Insulin Granules in Primary Cultured Beta Cells
   For the recombinant adenovirus production of insulin–GFP, a cDNA fragment containing pre-proinsulin and GFP was cut by *Eco*RI and *Not*I restriction enzymes, which was ligated into the pAdex1CA cosmid vector, and Adex1CA insulin–GFP was prepared and amplified by the standard protocol (Takara Shuzo Co., Kyoto, Japan) as described previously [40]. The reverse primer used here encodes the C-terminus of pre-pro-insulin, ending LENYCNWD. The fusion with the N-terminus of eGFP includes a short linker (provided by the pEGFP-N1 plasmid) such that the sequence reads LENYCNWDPPVATM (the linker sequence is underlined and M is the first residue of eGFP) [39].

2.2.2 Cell Culture

1. MIN6 cells
   - MIN6 cells (a gift from Prof. J.-I. Miyazaki (Osaka University, Osaka, Japan)) [41].
   - DMEM (Dulbecco's modified Eagle's MEM, high glucose) supplemented with 10 % fetal bovine serum (FBS), 50 units/ml penicillin, 50 μg/ml streptomycin, 28.4 μM 2-mercaptoethanol (GIBCO, Carlsbad, CA, USA).
   - Trypsin–EDTA: 0.25 % trypsin with 1 mM EDTA (ethylenediaminetetraacetic acid) solution (GIBCO).
   - PBS (phosphate buffered saline, pH 7.4, without $CaCl_2$, without $MgCl_2$).
   - Fibronectin (KOKEN, Tokyo, Japan).
   - Effectene transfection reagent (Qiagen, Hilden, Germany) (**Note 2**).
   - Coverglass: High-refractive-index ($n_d = 1.788$) coverglass (Olympus). Coverglass were treated with fibronectin in PBS for 15 min.
2. Primary Cultured pancreatic beta cells
   - C57BL/6 mice age 10–14 weeks (**Note 3**).
   - RPMI1640 medium (11 mM glucose, GIBCO/Invitrogen) supplemented with 10 % fetal bovine serum (FBS), 200 units/ml penicillin, 200 μg/ml streptomycin.

- Hank's balanced salt solution (HBSS, GIBCO/Invitrogen).
- Ca^{2+}-free KRB (Krebs-Ringer buffer; containing 1 mM EDTA).
- Liberase RI (Roche, Mannheim, Germany).
- Fibronectin (KOKEN, Tokyo, Japan).
- High-refractive-index (n_d=1.788) coverglass (Olympus) treated with fibronectin in PBS for 15 min.

2.2.3 Buffers and Reagents for Live Cell TIRF Imaging

1. Low-glucose KRB: KRB (110 mM NaCl, 4.4 mM KCl, 1.45 mM KH_2PO_4, 1.2 mM $MgSO_4$, 2.3 mM calcium gluconate, 4.8 mM $NaHCO_3$, 2.2 mM glucose, 10 mM HEPES, 0.3 % BSA; pH 7.4) was prepared.
2. High-glucose KRB: KRB (glucose concentration was changed to 22 mM) was prepared.
3. High KCl–KRB (NaCl was reduced to maintain the isotonicity of the solution) was prepared.
4. Immersion oil: Diiodomethane sulfur immersion oil (n_d = 1.78, Cargille Laboratories, NJ) was used to make contact between the objective lens and the coverslip (**Note 4**).

2.2.4 Buffers and Reagents for Fixed Cell TIRF Imaging

1. Paraformaldehyde buffer (0.1 M phosphate buffer, pH 7.4 with 4 % paraformaldehyde (Wako Pure Chemical Industries, Osaka, Japan)) was prepared.
2. Low-glucose KRB (Sect. 2.2.3) was prepared.
3. Blocking buffer (PBS with 3 % BSA (Free HG, Wako) and 0.1 % Triton X-100 (Surfact-Amps, Thermo, IL, USA)) was prepared.
4. Mounting media (PBS), 50 % Glycerol (Sigma-Aldrich), 2.5 % DABCO (1,4-diazabicyclo[2.2.2]octane, Sigma-Aldrich) was prepared.

2.2.5 Culture and Transfection to MIN6 Cells

1. MIN6 cells were seeded in a T-75 plastic flask, incubated in an atmosphere of 5 % CO_2 at 37 °C, and subcultured by regular trypsinization (wash with PBS and treatment with Trypsin–EDTA) and reseeding. For TIRF observation, cells were seeded on fibronectin-coated high-refractive-index coverglass.
2. MIN6 cells were transfected with insulin–GFP vector using Effectene transfection reagent according to the manufacturer's protocol. All experiments were performed between 2 and 3 days after transfection.

2.2.6 Culture and Adenoviral Infection to Primary Beta Cells

1. Preparation of beta cells: Pancreatic islets of Langerhans were isolated as described previously [42]. In brief, islets were isolated by collagenase (Liberase) digestion of C57BL/6 mouse pancreas and selected by handpicking. Isolated islets were

dissociated into single cells by incubation in Ca^{2+}-free KRB and cultured on fibronectin-coated high-refractive-index glass coverglass in RPMI1640 at 37 °C, in an atmosphere of 95 % air/5 % CO_2.

2. Infection: For the infection of the pancreatic beta cells with the recombinant adenovirus, 1-day cultured single cells were incubated with RPMI1640 medium (5 % FBS) and the required adenovirus (Adex1CA insulin–GFP: 30 multiplicity of infection per cell) for 1 h at 37 °C, after which RPMI1640 medium with 10 % FBS was added. All experiments were performed between 1 and 2 days after infection.

2.3 Methods

2.3.1 TIRF Microscopy System

Two types TIRF microscopy have been developed: prism-type TIRF microscopy and objective-type (through-the-lens-type) TIRF microscopy. The prism-type TIRF microscopy is mostly homemade setup. This setup is easily accomplished, since it requires only the microscope, prism, and laser, all components that are readily available. The drawback for this setup is the requirement that the specimen be positioned between the prism and the microscope objective, making it difficult to perform manipulations, to inject media into the specimen space, and to carry out physiological measurements. Recently, objective-type TIRF microscopy generates the evanescent field with the objective lens that is used for viewing the cell. The objective-type microscopes have been commercially available from Olympus, Nikon, and Zeiss Co. This setup requires that the laser be introduced through the microscope and greatly benefits from an objective lens with a numerical aperture (NA) >1.4. The specimen must be located on the top surface of the coverglass. The preparation, facing away from the objective, is accessible and permits the use of other instrumentation such as micromanipulators. We describe the objective-type TIRF microscopy system used in our laboratory (Fig. 7). This system is based on an Olympus objective-type TIRF microscope with minor modifications.

1. Light from an Ar laser (488 nm: Melles Griot, Carlsbad, CA) or a He/Ne laser (543 nm: Melles Griot) was introduced to an inverted microscope (IX70, Olympus Co., Tokyo, Japan) through a single-mode fiber and two illumination lenses; the light was focused at the back focal plane of a high-aperture objective lens (Apo 100× OHR; numerical aperture (NA) 1.65, Olympus) (**Note 5**). The focal point was moved off-axis to the most peripheral position in the objective lens by simply shifting the position of the fiber using micrometer laser adjustment.
2. To observe GFP alone, we used a 488-nm laser line for excitation and a 515-nm long-pass filter for the barrier. To observe the fluorescent image of RFP or Cy3, we used a 543-nm laser

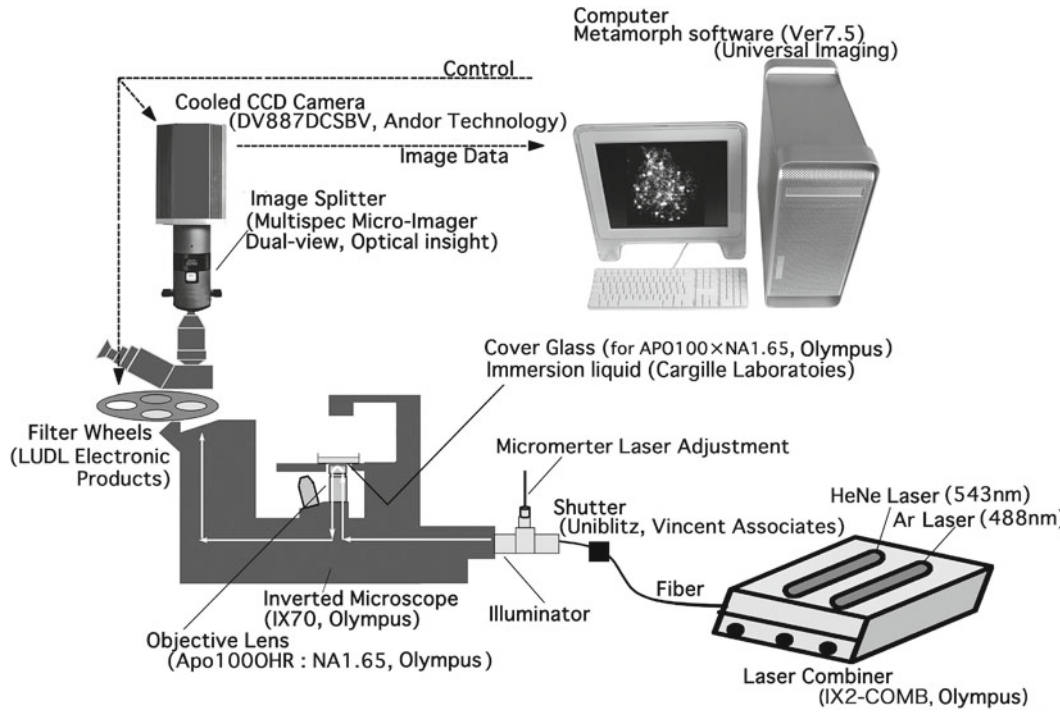

Fig. 7 Schematic representation of the TIRF setup described in the text

line and a long-pass 590-nm filter (Chroma, Brattleboro, VT). Two lasers can be introduced simultaneously with the laser combiner unit (Olympus). A filter wheel system (LUDL Electronic Products, Hawthorne, NY) is used with several interchangeable filters that can be rotated to bring the appropriate filter into the light path in a synchronized fashion. A computer-controlled shutter (Uniblitz, Vincent Associates, Rochester, NY) is placed between the laser combiner unit and illuminator to prevent photobleaching of cells between exposures.

3. Images were collected by a cooled charge-coupled device (CCD) camera (DV887DCSBV, ANDOR Technology, Belfast, Northern Ireland; operated with Metamorph version 7.5, Universal Imaging Corporation, Downingtown, PA) (**Note 6**). Images were acquired at 50–300-ms intervals.
4. To observe the fluorescence image of GFP and Cy3 simultaneously under TIRF illumination, we used the 488-nm laser line for excitation and an image splitter (Dual-View, MultiSpec Micro-Imager, Optical Insight, Santa Fe, NM) that divided the green and red components of the images with 565-nm dichroic mirror (Chroma) and passed the green component through a 530 ± 15-nm band-pass filter (Chroma) and the red

component through a 630 ± 25-nm band-pass filter or a 630-nm< long-pass filter (Chroma) (**Note 7**). Images were then projected side by side onto the CCD camera. The two images were brought into focus in the same plane by adding weak lenses to one channel, and they were brought into register by careful adjustment of the mirrors in the image splitter [43, 44]. Before each experimental session, we took an alignment image that showed the density by means of scattered 90-nm TetraSpeck fluorescent beads (Molecular Probes, Eugene, OR). They were visible in both the green and red channels and thus provided markers in the *x*–*y* plane. Beads in the two images were brought into superposition by shifting one image using Metamorph software.

5. Most analyses, including tracking (single projection of difference images) and area calculations, were performed using Metamorph software.

2.3.2 Live Cell TIRF Imaging

1. Turn TIRF system on 30 min before use.
2. Mount the insulin–GFP-transfected MIN6 cells or infected beta cells on the high-refractive-index coverslips in an open chamber and incubated in low-glucose KRB for 30 min at 37 °C.
3. Transfer coverslips to the thermostat-controlled stage (37 °C) of the TIRF microscope.
4. Find insulin–GFP expressing cells in epifluorescence first.
5. Incline of optic fiber of TIRF microscopy is switched from epifluorescent illumination mode to evanescent wave illumination mode using micrometer laser adjustment.
6. Precisely focus the image with z focus drive.
7. Lower laser intensity and use ND (neutral density) filters to minimize photodamage and increase CCD sensitivity/gain and image contrast.
8. Use Metamorph software to acquire images at 50–300-ms intervals.
9. Stimulate cells by switching buffers in a mounted chamber from low-glucose KRB to high-glucose KRB or high KCl–KRB. For bath application, stimulation with glucose and KCl was achieved by addition of 52 mM glucose–KRB or 100 mM KCl–KRB into the chamber (final = 50 mM KCl or 22 mM glucose).
10. Continue acquiring images for 20 min after high-glucose stimulation.
11. Save the acquired images to hard disk drive on a computer or to other physical media.

2.3.3 Analysis of Images

Most analyses, including tracking and area calculations, are performed using MetaMorph software. To analyze the data, fusion events are manually selected and the average fluorescence intensity of individual granules in a 1-μm × 1-μm square placed over the granule center is calculated. The number of fusion events is manually counted while looping 6,000 frame time lapses. Sequences are exported as single TIFF files or converted into AVI or QuickTime movies.

2.3.4 Fixed Cell TIRF Imaging

To look at docked insulin granules and endogenous protein in plasma membrane, we have used fixed cell TIRF imaging:

1. Culture primary beta cells or MIN6 cells on high-refractive-index glass coverglass.
2. Wash twice with low-glucose KRB.
3. Fix with 4 % paraformaldehyde for 15 min at room temperature.
4. Wash 3× 5 min with PBS.
5. When you image a fluorescent protein-expressing cells, skip to Section 2.3.4.11.
6. Block and permeabilize with blocking buffer (PBS with 3 % BSA and 0.1 % Triton X-100).
7. Incubate cells overnight at 4 °C with diluted primary antibodies.
8. Wash 3× 5 min with PBS.
9. Incubate cells for 1 h at room temperature in the dark with corresponding fluorescent-labeled secondary antibody conjugates.
10. Wash 3× 5 min with PBS.
11. To mount cells, mount media (PBS, 50 % Glycerol, 2.5 % DABCO) onto the cells on coverslip. Mounted slides should be stored at 4 °C protected from light.
12. Acquire images using TIRF microscopy.

2.3.5 Example of Insulin Exocytosis Imaging by TIRF

Beta cells release insulin on glucose stimulation with a biphasic pattern that consists of a rapidly initiated and transient first phase followed by a sustained second phase. TIRF imaging has allowed us to directly observe the dynamic motion of single insulin granules undergoing exocytosis during biphasic insulin release in living beta cells. We transfected mouse primary pancreatic beta cells with recombinant adenovirus encoding insulin–GFP in order to label the insulin secretory granules and then examined the dynamic motion of granules near the plasma membrane [45].

TIRF microscopy revealed that glucose stimulation induced interesting exocytotic responses that originated from two distinct

types of insulin granules with completely different behaviors prior to fusion: previously docked granules that are visible before the onset of stimulation under TIRF microscopy and newcomer granules that cannot be detected by TIRF microscopy or are dimly visible before stimulation (Fig. 8a). It should be noted that in primary cultured pancreatic beta cells, newcomer granules fuse immediately after they reach the plasma membrane. The time from landing to fusion is less than 50 ms [39]. More interestingly, these two types of fusion events reveal different temporal patterns. Fusions originating from previously docked granules are detected preferentially during the first phase, whereas fusion events during the second phase mostly arose from newcomer granules (Fig. 8b). Thus, it is likely that there is a mechanistic difference between first and second phase release [39, 45].

We also examined the relationship between t-SNARE syntaxin 1A and biphasic insulin release by TIRF microscopy [45]. Syntaxin 1A was shown to play a crucial role in secretory granule docking and subsequent fusion steps in the exocytotic process. We examined the docking status of insulin granules in syntaxin 1A-knockout (syntaxin $1A^{-/-}$) beta cells using fixed cell TIRF imaging with immunostaining for insulin (Fig. 8c). We interpret the individual fluorescent spots shown in the TIRF image in Fig. 8c to be equivalent to morphologically docked granules. We rarely observed morphologically docked granules in syntaxin $1A^{-/-}$ cells. In live cell beta-cell TIRF imaging, syntaxin $1A^{-/-}$ mice beta cells showed fewer previously docked granules with no fusion during the first phase, whereas fusion from newcomers, which are responsible for second phase release, was still preserved (Fig. 8d, e). Thus, we proposed a model for biphasic insulin release wherein docking and fusion of insulin granules is Synt1A-dependent during the first phase but Synt1A-independent during the second phase [45].

3 Notes

1. GFP-tagged neuropeptide Y, phogrin, and IAPP were also used to label insulin granules [46–48].
2. We have also used Lipofectamine 2000 (Life Technologies, Carlsbad, CA).
3. We have also used Wistar rats age 8–10.
4. In order to maintain the NA (1.65) and to achieve the high quality of image, a special coverglass of high-refractive-index glass ($n_d = 1.788$, Olympus) and special immersion medium of high refractive index (immersion liquid: $n_d = 1.78$, Cargille Laboratories) must be used.
5. We use a high-aperture objective lens (Olympus APO 100×/NA 1.65 apochromatic objective lens). Living cells typically have a refractive index about 1.37. To achieve total internal

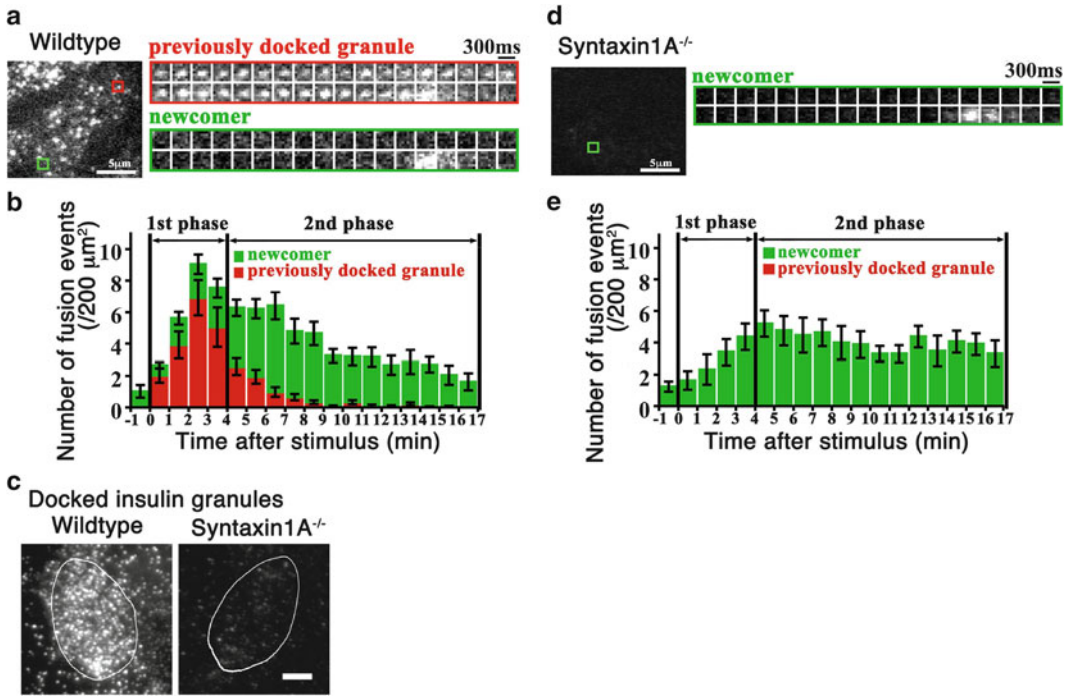

Fig. 8 TIRF images and analysis of single GFP-labeled insulin granule motion in mouse primary beta cells during glucose stimulation. (**a**) *Left panel*: The real-time motion of GFP-labeled insulin granules in WT beta cell was imaged to the plasma membrane. This is the TIRF image of a single cell harboring insulin–GFP, showing that many insulin granules docked to the plasma membrane. *Right panel*: Sequential images (1 μm × 1 μm per 300-ms interval) of a granule docking and fusing with the plasma membrane were presented during 22-mM glucose stimulation. (**b**) Histogram of the number of fusion events (per 200 μm²) in WT β-cells at 60-s intervals after stimulation ($n = 10$ cells). The *black column* shows fusion from previously docked granules, and the *gray column* shows fusion from newcomers. During the first phase, fusion occurred mostly from previously docked granules. (**c**) TIRF images of docked insulin granules in WT or Synt1A$^{-/-}$ β-cells (fixed cell TIRF imaging). The surrounding *lines* represent the outline of cells that attached to the coverglass. Scale bar: 5 μm. Pancreatic β-cells were prepared from WT and Synt1A$^{-/-}$ mice, fixed, and immunostained for insulin. (**d**) TIRFM during glucose stimulation in Synt1A$^{-/-}$ β-cells and sequential images of a newcomer granule docking and fusing under glucose stimulation. (**e**) Histogram of the number of fusion events (per 200 μm²) in the Synt1A$^{-/-}$ cells at 60-s intervals after stimulation (modified from our previous data [45])

reflection, such a specimen must be illuminated with NA greater than 1.37. Recently, 1.4–1.45 NA objectives using normal coverglass and immersion oil have been available from Olympus, Nikon, and Zeiss Co.

6. Underlying all direct imaging of living cells is the desire to preserve the living subject for as long as possible, through minimization of both phototoxic cell damage and also photobleaching of the incorporated fluorophores. Higher sensitive CCD (Electron Multiplying CCD) is suitable for TIRF microscopy system, which not only exhibits the sensitivity and speed to capture dynamic membrane events from within very thin small excitation volume but furthermore enables the laser excitation power to be attenuated.

7. The penetration depth is dependent on the wavelength (λ). To precisely analyze the colocalization of GFP and RFP/Cy3, we only use the 488-nm laser line for excitation. However, the fluorescence intensity of red component by 488-nm excitation is relatively low compared to that by 543-nm excitation. Recently, multicolor, multi-angle illuminator that allows simultaneous multi-channel laser TIRF illumination, has been available from Olympus (RFAEVAW, Cell TIRF). Users can control each laser's penetration depth to simultaneously capture TIRF for multi-channels.

References

1. Mahato RI, Henry J, Narang AS, Sabek O, Fraga Ashcroft SJ, Bunce J, Lowry M, Hansen SE, Hedeskov CJ (1978) The effect of sugars on (pro)insulin biosynthesis. Biochem J 174:517–526
2. Hedeskov CJ (1980) Mechanism of glucose-induced insulin secretion. Physiol Rev 60:442–509
3. Welsh M, Nielsen DA, MacKrell AJ, Steiner DF (1985) Control of insulin gene expression in pancreatic beta-cells and in an insulin-producing cell line, RIN-5F cells. II. Regulation of insulin mRNA stability. J Biol Chem 260:13590–13594
4. Welsh M, Scherberg N, Gilmore R, Steiner DF (1986) Translational control of insulin biosynthesis. Evidence for regulation of elongation, initiation and signal-recognition-particle-mediated translational arrest by glucose. Biochem J 235:459–467
5. Newgard CB, McGarry JD (1995) Metabolic coupling factors in pancreatic beta-cell signal transduction. Annu Rev Biochem 64:689–719
6. Nagamatsu S (2008) Mechanism of insulin exocytosis analysed by imaging techniques. In: Seino S, Bell GI (eds) Pancreatic beta cells in health and disease. Springer, pp 177–194
7. Greider MH, Howell SL, Lacy PE (1969) Isolation and properties of secretory granules from rat islets of Langerhans. II. Ultrastructure of the beta granule. J Cell Biol 41:162–166
8. Lange RH (1974) Crystalline islet B-granules in the grass snake (*Natrix natrix* (L.)): tilting experiments in the electron microscope. J Ultrastruct Res 46:301–307
9. Wollheim CB, Lang J, Regazzi R (1996) The exocytotic process of insulin secretion and its regulation by Ca^{2+} and G-proteins. Diabetes Rev 4:276– 297
10. Regazzi R, Wollheim CB, Lang J, Theler JM, Rossetto O, Montecucco C, Sadoul K, Weller U, Palmer M, Thorens B (1995) VAMP-2 and cellubrevin are expressed in pancreatic beta-cells and are essential for Ca(2+)-but not for GTP gamma S-induced insulin secretion. EMBO J 14:2723–2730
11. Sadoul K, Lang J, Montecucco C, Weller U, Regazzi R, Catsicas S, Wollheim CB, Halban PA (1995) SNAP-25 is expressed in islets of Langerhans and is involved in insulin release. J Cell Biol 128:1019–1028
12. Boyd RS, Duggan MJ, Shone CC, Foster KA (1995) The effect of botulinum neurotoxins on the release of insulin from the insulinoma cell lines HIT-15 and RINm5F. J Biol Chem 270:18216–18218
13. Nagamatsu S, Fujiwara T, Nakamichi Y, Watanabe T, Katahira H, Sawa H, Akagawa K (1996) Expression and functional role of syntaxin 1/HPC-1 in pancreatic beta cells. Syntaxin 1A, but not 1B, plays a negative role in regulatory insulin release pathway. J Biol Chem 271:1160–1165
14. Nagamatsu S, Nakamichi Y, Yamamura C, Matsushima S, Watanabe T, Ozawa S, Furukawa H, Ishida H (1999) Decreased expression of t-SNARE, syntaxin 1, and SNAP-25 in pancreatic beta-cells is involved in impaired insulin secretion from diabetic GK rat islets: restoration of decreased t-SNARE proteins improves impaired insulin secretion. Diabetes 48:2367–2373
15. Ohara-Imaizumi M, Nishiwaki C, Nakamichi Y, Kikuta T, Nagai S, Nagamatsu S (2004) Correlation of syntaxin-1 and SNAP-25 clusters with docking and fusion of insulin granules analysed by total internal reflection fluorescence microscopy. Diabetologia 47:2200–2207
16. Ju Q, Edelstein D, Brendel MD, Brandhorst D, Bretzel RG, Brownlee M (1998) Transduction of non-dividing adult human pancreatic beta cells by an integrating lentiviral vector. Diabetologia 41:736–739
17. Flotte T, Agarwal A, Wang J, Song S, Fenjves ES, Inverardi L, Chesnut K, Afione S, Loiler S,

Wasserfall C, Kapturczak M, Ellis T, Nick H, Atkinson M (2001) Efficient ex vivo transduction of pancreatic islet cells with recombinant adeno-associated virus vectors. Diabetes 50:515–520

18. Ceste ME, Afra R, Mullen Y, Drazan KE, Benhamou PY, Shaked A (1994) Adenoviral-mediated gene transfer to pancreatic islets does not alter islet function. Transplant Proc 6:1545–1551
19. Wick PF, Senter RA, Parsels LA, Uhler MD, Holz RW (1993) Transient transfection studies of secretion in bovine chromaffin cells and PC12 cells. Generation of kainate-sensitive chromaffin cells. J Biol Chem 268: 10983–10989
20. Coppola T, Perret-Menoud V, Lüthi S, Farnsworth CC, Glomset JA, Regazzi R (1999) Disruption of Rab3-calmodulin interaction, but not other effector interactions, prevents Rab3 inhibition of exocytosis. EMBO J 18:5885–5891
21. Iezzi M, Regazzi R, Wollheim CB (2000) The Rab3-interacting molecule RIM is expressed in pancreatic beta-cells and is implicated in insulin exocytosis. FEBS Lett 474:66–70
22. Mahato RI, Henry J, Narang AS, Sabek O, Fraga D, Kotb M, Gaber AO (2003) Cationic lipid and polymer-based gene delivery to human pancreatic islets. Mol Ther 7:89–100
23. Lakey JR, Young AT, Pardue D, Calvin S, Albertson TE, Jacobson L, Cavanagh TJ (2001) Nonviral transfection of intact pancreatic islets. Cell Transplant 10:697–708
24. Gainer AL, Korbutt GS, Rajotte RV, Warnock GL, Elliott JF (1996) Successful biolistic transformation of mouse pancreatic islets while preserving cellular function. Transplantation 61:1567–1571
25. Cabrera O, Berman DM, Kenyon NS, Ricordi C, Berggren PO, Caicedo A (2006) The unique cytoarchitecture of human pancreatic islets has implications for islet cell function. Proc Natl Acad Sci U S A 103:2334–2339
26. Straub SG, Sharp GW (2002) Glucose-stimulated signaling pathways in biphasic insulin secretion. Diabetes Metab Res Rev 18:451–463
27. Rorsman P, Renstrom E (2003) Insulin granule dynamics in pancreatic beta cells. Diabetologia 46:1029–1045
28. Axerlod D (2001) Total internal reflection fluorescence microscopy in cell biology. Traffic 2:764–774
29. Steyer JA, Almers W (2001) A real-time view of life within 100 nm of the plasma membrane. Nat Rev Mol Cell Biol 2:268–275
30. Axelrod D (1981) Cell-substrate contacts illuminated by total internal reflection fluorescence. J Cell Biol 89:141–145
31. Truskey GA, Burmeister JS, Grapa E, Reichert WM (1992) Total internal reflection fluorescence microscopy (TIRFM). II. Topographical mapping of relative cell/substratum separation distances. J Cell Sci 103:491–499
32. Vale RD, Funatsu T, Pierce DW, Romberg L, Harada Y, Yanagida T (1996) Direct observation of single kinesin molecules moving along microtubules. Nature 380:451–453
33. Sund SE, Axelrod D (2000) Actin dynamics at the living cell submembrane imaged by total internal reflection fluorescence photobleaching. Biophys J 79:1655–1669
34. Dickson RM, Norris DJ, Tzeng YL, Moerner WE (1996) Three-dimensional imaging of single molecules solvated in pores of poly(acrylamide) gels. Science 274:966–969
35. Oheim M, Loerke D, Stühmer W, Chow RH (1998) The last few milliseconds in the life of a secretory granule. Docking, dynamics and fusion visualized by total internal reflection fluorescence microscopy (TIRFM). Eur Biophys J 27:83–98
36. Sako Y, Minoghchi S, Yanagida T (2000) Single-molecule imaging of EGFR signalling on the surface of living cells. Nat Cell Biol 2:168–172
37. Tsuboi T, Zhao C, Terakawa S, Rutter GA (2000) Simultaneous evanescent wave imaging of insulin vesicle membrane and cargo during a single exocytotic event. Curr Biol 10:1307–1310
38. Ohara-Imaizumi M, Nakamichi Y, Tanaka T, Ishida H, Nagamatsu S (2002) Imaging exocytosis of single insulin secretory granules with evanescent wave microscopy: distinct behavior of granule motion in biphasic insulin release. J Biol Chem 277:3805–3808
39. Ohara-Imaizumi M, Nishiwaki C, Kikuta T, Nagai S, Nakamichi Y, Nagamatsu S (2004) TIRF imaging of docking and fusion of single insulin granule motion in primary rat pancreatic beta-cells: different behaviour of granule motion between normal and Goto-Kakizaki diabetic rat beta-cells. Biochem J 381:13–18
40. Nagamatsu S, Watanabe T, Nakamichi Y, Yamamura C, Tsuzuki K, Matsushima S (1999) α-Soluble N-ethylmaleimide-sensitive factor attachment protein is expressed in pancreatic β -cells and functions in insulin, but not γ -amino butyric acid secretion. J Biol Chem 274:8053–8060
41. Miyazaki J-I, Araki K, Yamato E, Ikegami H, Asano T, Shibasaki Y, Oka Y, Yamamura K-I (1990) Establishment of a pancreatic beta cell line that retains glucose-inducible insulin secretion: special reference to expression of

glucose transporter isoforms. Endocrinology 127:126–132

42. Lacy PE, Kostianovsky M (1967) Method for the isolation of intact islet of Langerhans from the rat pancreas. Diabetes 16:35–39
43. Ohara-Imaizumi M, Nishiwaki C, Kikuta T, Kumakura K, Nakamichi Y, Nagamatsu S (2004) Site of docking and fusion of insulin secretory granules in live MIN6 beta cells analyzed by TAT-conjugated anti-syntaxin 1 antibody and total internal reflection fluorescence microscopy. J Biol Chem 279:8403–8408
44. Ohara-Imaizumi M, Ohtsuka T, Matsushima S, Akimoto Y, Nishiwaki C, Nakamichi Y, Kikuta T, Nagai S, Kawakami H, Watanabe T, Nagamatsu S (2005) ELKS, a protein structurally related to the active zone-associated protein CAST, is expressed in pancreatic beta cells and functions in insulin exocytosis: interaction of ELKS with exocytotic microscopy. Mol Biol Cell 16:3289–3300
45. Ohara-Imaizumi M, Fujiwara T, Nakamichi Y, Okamura T, Akimoto Y et al (2007) Imaging analysis reveals mechanistic differences between first- and second-phase insulin exocytosis. J Cell Biol 177:695–705
46. Pouli AE, Emmanouilidou E, Zhao C, Wasmeier C, Hutton JC, Rutter GA (1998) Secretory-granule dynamics visualized in vivo with a phogrin-green fluorescent protein chimaera. Biochem J 333:193–199
47. Tsuboi T, Rutter GA (2003) Multiple forms of "kiss-and-run" exocytosis revealed by evanescent wave microscopy. Curr Biol 13:563–567
48. Michael DJ, Xiong W, Geng X, Drain P, Chow RH (2007) Human insulin vesicle dynamics during pulsatile secretion. Diabetes 56:1277–1288